The Human Islet Amyloid Polypeptide Forms Transient Membrane-Active Prefibrillar Assemblies†

Yair Porat,‡ Sofiya Kolusheva,§ Raz Jelinek,§ and Ehud Gazit*,‡

Department of Molecular Microbiology and Biotechnology, George S. Wise Faculty of Life Sciences, Tel-Aviv University, Tel-Aviv 69978, Israel, and Department of Chemistry, Ben Gurion University of the Negev, Beersheva 84105, Israel

Received May 26, 2003; Revised Manuscript Received July 28, 2003

ABSTRACT: The formation of amyloid fibrils by the human islet amyloid polypeptide is associated with type II diabetes. While it was previously suggested that the formed fibrils are toxic to pancreatic β-cells due to membrane permeation activity, more recent studies suggested that protofibrillar assemblies have significantly higher potency in permeating lipid bilayers. Here, we specifically studied the membrane interaction activity of soluble and insoluble islet amyloid polypeptide assemblies at high temporal resolution. A colorimetric analysis using lipid/polydiacetylene (PDA) biomimetic vesicles clearly demonstrated the transient formation of soluble assemblies that strongly interact with the lipid vesicles. A peak in the level of membrane binding of the soluble fraction, as reflected by the colorimetric assay, was observed after incubation for ~1 h, followed by a decrease in the level of membrane interaction of the assemblies. The transient nature of the membrane-active assemblies was independently confirmed by a fluorescence quenching assay. Ultrastructural analysis using transmission electron microscopy provided morphological evidence of prefibrillar assemblies, supported the transient existence of membrane interacting soluble species, and facilitated observation of the non-membrane-active filaments in the solution. Taken together, our results provide experimental evidence for the formation of transient soluble prefibrillar assemblies which are highly membrane-active. The implications of these observations are discussed in light of designed fibrillization inhibitors.

Formation of ordered amyloid fibrils has been detected in a number of diseases of unrelated origin, including Alzheimer's disease, Parkinson's disease, prion diseases (such as the bovine spongiform encephalopathy), and type II diabetes (*1*−*5*). Type II diabetes, one of the most common amyloid-related diseases, is characterized by pancreatic amyloid deposits in more than 90% of diabetic patients (*6*). These deposits are composed of the islet amyloid polypeptide (IAPP),[1] a 37-residue peptide hormone that is produced in the pancreatic β cells and cosecreted with insulin. The early stage of type II diabetes is characterized by insulin resistance, followed by increased insulin and IAPP secretion. This secretion initiates an increase in extracellular IAPP concentrations that may exceed 100-fold of the normal IAPP concentration (*7*−*9*). The elevated concentration is probably a key issue in amyloid formation as fibril assembly is nucleation-dependent, and the lag time needed for the nucleation of amyloid fibrils growth is strongly correlated with protein concentration (*10*−*13*).

While the mechanism of amyloid fibril assembly is not fully understood, the appearance of disease-related fibril aggregates has been correlated with potent nonspecific cytotoxicity. Furthermore, assemblies of non-disease-related amyloid fibril structures were also shown to induce significant cytotoxic effects (*14*). In that regard, membrane permeation was proposed as a primary mechanism mediating amyloid fibril cytotoxicity, which might explain the generic and non-receptor-specific activities of such assemblies (*1*−*6*).

In the case of human IAPP (hIAPP), even though a direct correlation between hIAPP fibrillization and *in vivo* β cell death has not yet been fully established, several studies have shown that external addition of synthetic hIAPP at low concentrations (8−10 μM) induced cytotoxic death in cell culture (*15*−*18*). A later study indicated that protofibrillar hIAPP, rather than fibrillar hIAPP, permeabilized model lipid vesicles (*19*). Protofibrillar intermediates are known to exist not only in the case of hIAPP but also in the early stages of fibril formation of various amyloidogenic proteins such as β-amyloid, α-synuclein, ABri peptide, and the N-terminal domain of HypF protein (*20*−*23*). These soluble assemblies are rich in β-sheet structures and share similar radial dimensions of 7−12 nm (*20*). The protofibrils are transient and eventually disappear as mature fibrils grow. A recent study suggested that soluble amyloid oligomers consisting

† This research was supported by a start-up grant from the U.S.-Israel Binational Science Foundation (BSF-2000337) and the Dan David Scholarship Award to E.G.

* To whom correspondence should be addressed: Department of Molecular Microbiology and Biotechnology, Tel-Aviv University, Tel-Aviv 69978, Israel. E-mail: ehudg@post.tau.ac.il. Telephone: +972-3-640-9030. Fax: +972-3-640-5448.

‡ Tel-Aviv University.

§ Ben Gurion University of the Negev.

[1] Abbreviations: CD, circular dichroism; CR, colorimetric response; HFIP, 1,1,1,3,3,3-hexafluoro-2-propanol; hIAPP, human islet amyloid polypeptide; IAPP, islet amyloid polypeptide; NBD, 7-nitrobenz-2-oxa-1,3-diazole; PC, phosphatidylcholine; PDA, polydiacetylene; PE, phosphatidylethanolamine; TEM, transmission electron microscopy; HR-TEM, high-resolution TEM.

10.1021/bi034889i CCC: $25.00
Published on Web 08/23/2003

of diverse proteins might share a common structure (*24*). This hypothesis was due to the fact that antibodies, raised to specifically recognize micellar structures of Alzheimer's Aβ polypeptide, but not its soluble or amyloid forms, interacted with soluble oligomer assemblies of structurally unrelated proteins such as insulin, IAPP, polyglutamine, and α-synuclein, and inhibited their cytotoxic effect (*24*).

One of the crucial questions pertaining to the biological activity of protofibrils concerns the extent of their membrane interactions and significant cytotoxic effects. Here, we study membrane binding and ultrastructures of soluble and nonsoluble hIAPP assemblies at high temporal resolution. Application of a colorimetric lipid/polydiacetylene vesicle assay, facilitating evaluation of peptide−membrane interactions (*25*−*27*), revealed that the association of hIAPP monomers into membrane-reactive soluble prefibrillar assemblies is rapid and transient in nature. The colorimetric analysis demonstrated that the prefibrillar assemblies rather than the amyloid fibrils were the predominant membrane-active species, and that the maximal level of bilayer binding occurring within 1 h rapidly declines thereafter. A fluorescence quenching assay using a bilayer probe independently confirmed the transient existence of the soluble, membrane-reactive assemblies. In addition, electron microscopy analysis allowed visualization of the lipid disruption effect caused by the prefibrillar assemblies and suggests that alteration of membrane morphology by the prefibrils is similar to the effects of membrane-permeating toxins.

EXPERIMENTAL PROCEDURES

Preparation of hIAPP Aggregates and Fraction Separation. Synthetic hIAPP (CalBiochem) was dissolved in HFIP (1.95 mg/mL) and diluted to a final concentration of 5 μM in 10 mM sodium acetate buffer (pH 6.5), and a final HFIP concentration of 1% (by volume). Immediately after dilution, and every 30 min, 1 mL samples solutions were transferred to a microtube and centrifuged for 15 min at 20000*g* and 4 °C. The supernatant fractions (0.6 mL) were transferred to another tube, and pellet fractions were gently resuspended in the remaining 0.4 mL. For the higher-temporal resolution experiments, the same procedure was used using 4 μM hIAPP in 10 mM sodium acetate buffer (pH 6.5) and a final HFIP concentration of 1% (by volume), at 20 min intervals.

Polymerized Lipid Vesicles. The diacetylene monomer tricosadiynoic acid was purchased from GFS Chemicals (Powell, OH). Dimyristoylphosphatidylcholine (DMPC) was purchased from Sigma (St. Louis, MO). Preparation of vesicles containing lipids and PDA has been described previously (*25*−*27*). Briefly, the phospholipid and monomer constituents were dissolved in chloroform and ethanol and dried together *in vacuo*, followed by addition of deionized water and probe sonication for 2−3 min at 70 °C. The vesicle solution was cooled and kept at 4 °C overnight, and then polymerized in an ultraviolet (UV) oven (cross-linker) by irradiation at 220 nm for 10−20 s. The resulting solutions exhibited an intense blue color.

Color Reaction Assay. Vesicles were prepared at total lipid concentrations of 1 mM. Samples for the colorimetric measurements were prepared by adding 100 μL of 5 μM hIAPP after centrifugal separation (or 4 μM in the higher-temporal resolution experiments, as described above) to 50 μL of 0.5 mM total lipid vesicles and diluted using 25 mM Tris base (pH 8) to a final volume of 1 mL. UV−vis measurements were carried out at 28 °C using a Jasco V550 UV−visible spectrophotometer, with a 1 cm optical path length cell. To quantify the extent of blue-to-red color transitions within the vesicle solutions, the colorimetric response (%CR) was defined and calculated as follows (*28*):

$$\%\mathrm{CR} = \frac{\mathrm{PB}_0 - \mathrm{PB}_\mathrm{I}}{\mathrm{PB}_0} \times 100$$

where $\mathrm{PB} = A_{\mathrm{blue}}/(A_{\mathrm{blue}} + A_{\mathrm{red}})$ and A is the absorbance at 640 nm, the "blue" component of the spectrum, or at 500 nm, the "red" component (blue and red refer to the visual appearance of the material, not the actual absorbance). PB_0 is the blue-to-red ratio of the control sample before induction of a color change by the added hIAPP peptide, and PB_I is the value obtained after the colorimetric transition induced by hIAPP.

NBD Fluorescence Quenching Assay. Vesicles containing NBD-PE were prepared as described in ref *29*. Briefly, C_6-NBD-PE was dissolved in chloroform, added to the monomers and phospholipids at 1 mol %, and dried together *in vacuo* before sonication (see Polymerized Lipid Vesicles). Addition of the NBD-labeled phospholipids did not affect either the blue color of the vesicles or the blue−red transitions.

Samples were prepared by adding 4 μM hIAPP, after centrifugal separation (as described above), to 0.5 mM total lipid vesicles and 25 mM Tris base (pH 8) to a final volume of 1 mL. The fluorescence quenching reaction was initiated by adding sodium dithionite from a stock solution (0.6 M), prepared in 50 mM Tris buffer (pH 11), to a final concentration of 10 mM. The decrease in fluorescence was monitored for 5 min at 28 °C using 467 nm excitation and 535 nm emission on an Edinburgh FL920 spectrofluorimeter. The fluorescence decay was calculated as a percentage of the initial fluorescence measured before the addition of dithionite. A control curve represented NBD fluorescence decays induced by dithionite only, while other curves were recorded following addition of hIAPP after different aggregation periods.

Transmission Electron Microscopy. Samples (10 μL) of hIAPP−phospholipid/PDA vesicle mixtures extracted for the colorimetric assay (both pellet suspension and supernatant) were placed on 400 mesh copper grids (SPI supplies, West Chester, PA) covered by carbon-stabilized Formvar film. After 1 min, excess fluid was removed, and the grids were negatively stained with 2% uranyl acetate in water for an additional 2 min. Samples were viewed with a JEOL 1200EX electron microscope operating at 80 kV and high-resolution Philips Tecnai F20 field emission gun TEM operating at 200 kV.

Circular Dichroism Spectroscopy. hIAPP (4 μM, 500 μL) was prepared as described above. hIAPP/lipid vesicle mixtures were prepared by adding 50 μL of lipid vesicles to 445 μL of acetate buffer, and finally, hIAPP in HFIP was added to a final concentration of 4 μM and a final volume of 500 μL. Spectra were recorded at 25 °C between 195 and 250 nm, with 1 nm intervals and a 4 s averaging time, using an AVIV 202 CD spectrometer. Final scan values represent subtraction of baseline (buffer in the case of hIAPP and

buffer with lipid/PDA vesicles for the peptide/vesicle mixtures) and smoothing using AVIV CDS version 2.73.

RESULTS

Studying the membrane interaction properties of hIAPP is crucial for the understanding of one of the most common amyloid-related cytotoxic effects. However, the aggregation of hIAPP is significantly more rapid than aggregation of other known amyloidogenic proteins such as α-synuclein or *β*-amyloid, which makes the analysis of membrane association difficult. Specifically, compared to fibrillization processes of days or even weeks observed for other amyloidogenic peptides, hIAPP fibrillization is completed in a few hours even at very low concentrations, and thus, the separation and extraction of putative membrane-active species by chromatography are impractical. Here we incubated hIAPP monomers at different durations and determined the membrane interaction profiles of the assembled aggregates using a biomimetic lipid/PDA vesicle assay. Colorimetric, fluorescence, and electron microscopy experiments facilitated high temporal resolution of the membrane-active species in the amyloid solutions.

Membrane Interactions of hIAPP Aggregates Using a Colorimetric Assay. To study the membrane interactions of the soluble and insoluble hIAPP assemblies, we recorded the color transitions induced by fibrils and prefibrils upon interaction with chromatic phosphatidylcholine (PC)/PDA vesicles (2:3 mole ratio). Lipid/PDA vesicles have been shown to serve as a versatile platform for detection and analysis of membrane interactions (*25*−*27*, *30*, *31*).

To initiate the aggregation process, synthetic hIAPP (5 *μ*M) was dissolved in 1% HFIP and 10 mM acetate buffer (pH 6.5). Within short intervals, nonsoluble aggregates were separated by centrifugation, and after addition of the soluble supernatants or the resuspended pellets to the lipid/PDA vesicle solutions, the induced colorimetric transitions were recorded.

Figure 1 demonstrates that a distinct difference in the induced colorimetric transitions was apparent between the supernatant and pellet of hIAPP. Specifically, an increase in the colorimetric response induced by the supernatant was observed, reaching a maximal %CR value after approximately 1 h, followed by a rapid decrease (Figure 1A). The blue−red color transformations induced by the suspended pellet, on the other hand, were small at all times, showing experimentally insignificant variations (Figure 1A).

To achieve higher temporal resolution, we repeated the colorimetric experiment using a slightly lower hIAPP concentration and shorter time intervals (Figure 1B). An almost identical trend of a transient increase in the extent of the color reaction was observed for the supernatant fractions with a maximal colorimetric response approximately 80 min after the initial peptide solubilization (Figure 1B). Again, the colorimetric changes induced by the resuspended pellets were consistently low for the duration of the measurements. The higher temporal resolution depicted in Figure 1B allowed a clear observation of a gradual rise in the level of membrane binding followed by a subsequent decrease in membrane activity. This result implies the formation and ensuing disappearance of transient membrane-active prefibrillar assemblies.

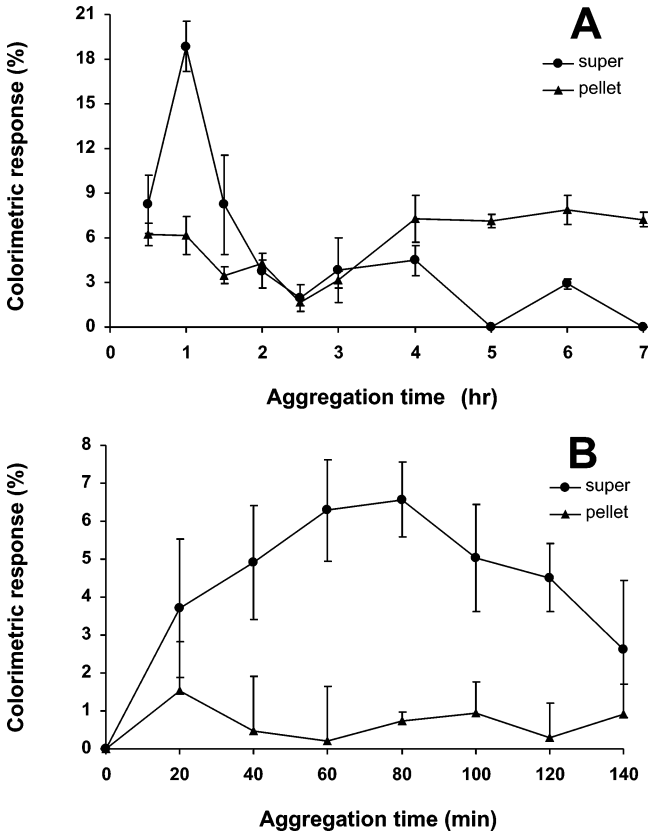

FIGURE 1: Membrane interaction of fibrils and prefibrillar assemblies using the colorimetric lipid/PDA vesicle assay. Human IAPP was dissolved in sodium acetate buffer and HFIP (1%). Fractions were separated using centrifugation and added separately to the vesicles in Tris-HCl (pH 8): (●) supernatant and (▲) pellet. Color response values were measured in three independent repeats, and error bars represent the standard deviation. (A) Color response of 5 *μ*M hIAPP fractions at 30 min intervals. A significant increase is observed for the supernatant fraction, which contains mostly prefibrils, within 1 h. (B) Same procedure as for panel A using 4 *μ*M hIAPP and 20 min intervals to enhance the temporal resolution of the colorimetric response.

Fluorescence Quenching of Bilayer Surface NBD. To confirm the existence of transient membrane-active assemblies of hIAPP, we carried out a fluorescence quenching experiment, utilizing C_6-NBD-PE incorporated within the phospholipid/PDA vesicles (Figure 2). In these experiments, we examined the effect of membrane-active species formed in the hIAPP suspensions upon the fluorescence quenching of C_6-NBD-PE by sodium dithionite (*32*). In principle, greater bilayer perturbation by membrane-reactive aggregates in solution would give rise to faster fluorescence quenching of the NBD label.

In the experiments depicted in Figure 2, samples of freshly dissolved hIAPP were prepared following centrifugation every 30 min and added to NBD-PE/DMPC/PDA (0.01:2:3 mole ratio) vesicles, and the quenching reaction was initiated by a reaction with sodium dithionite to a final concentration of 10 mM. The fluorescence emission at 535 nm was then monitored for 3.5 min. The fluorescence decays shown in Figure 2 are presented as a percentage of the initial fluorescence measured before addition of dithionite. The topmost decay curve in Figure 2 was recorded for the control sample (without adding peptide suspensions). The slower decay in the control vesicle solution was due to the slow

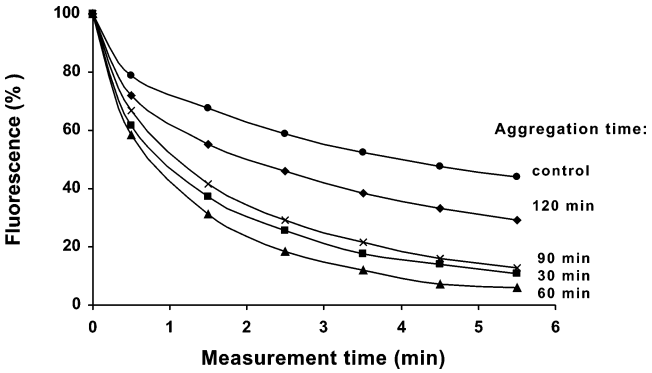

FIGURE 2: Lipid bilayer perturbation by hIAPP using the NBD marker. The NBD fluorescence was measured after addition of 4 μM hIAPP and the dithionite quencher, and fluorescence values represent the percentage of initial emission reading. The control curve represents the fluorescent decay without addition of hIAPP, while the other curves depict the fluorescence decays induced by supernatant fractions (containing mostly prefibrils) at various time points of aggregation. The maximum quenching effect was measured for the soluble fraction after incubation for 1 h.

penetration of the water-soluble dithionite quencher ion into the intact vesicles.

Faster fluorescence decays were observed when fractions of the supernatant suspensions were added to the NBD-PE/DMPC/PDA vesicles (Figure 2). Importantly, the most pronounced quenching occurred after addition of the supernatant fraction collected 60 min after dissolution of hIAPP (lowest curve in Figure 2). This enhanced quenching most likely corresponds to the better access of quencher molecules to the bilayer as a result of perturbation of the lipid surface by hIAPP prefibrils. As aggregation proceeded, the quenching rates became slower (Figure 2), consistent with fewer lipid interactions by the aggregating fibrils. Overall, the fluorescence quenching data shown in Figure 2 are consistent with the colorimetric analysis (Figure 1) and indicate that the most active membrane-reactive prefibrils assembled in the hIAPP solution after approximately 1 h. The fluorescence quenching data further demonstrate the existence of transient, stronger membrane binding soluble prefibrillar assemblies formed ~1 h after peptide incubation.

Ultrastructural TEM Visualization. To visualize the hIAPP assemblies and their effect on the phospholipid/PDA vesicles, an ultrastructural analysis was performed using TEM (Figures 3 and 4) and HR-TEM (Figure 4). The TEM images in Figure 3 show lipid/PDA vesicles mixed with hIAPP suspensions extracted at different times. In the experiments depicted in Figure 3, synthetic hIAPP was dissolved, separated using centrifugation, and mixed with the lipid/PDA vesicles as described in the colorimetric analysis (Figure 1). The samples were then negatively stained using uranyl acatate and analyzed by TEM.

Figure 3A features the control DMPC/PDA vesicle solution. The polymerized vesicles adopt elongated rectangle shapes due to the ordered PDA framework. Addition of an hIAPP supernatant fraction extracted 60 min after the initial dissolution of the peptide induced a significant degradation of the vesicles (Figure 3B). This result resembles the effect of mixing the DMPC/PDA vesicles with polymyxin B, a

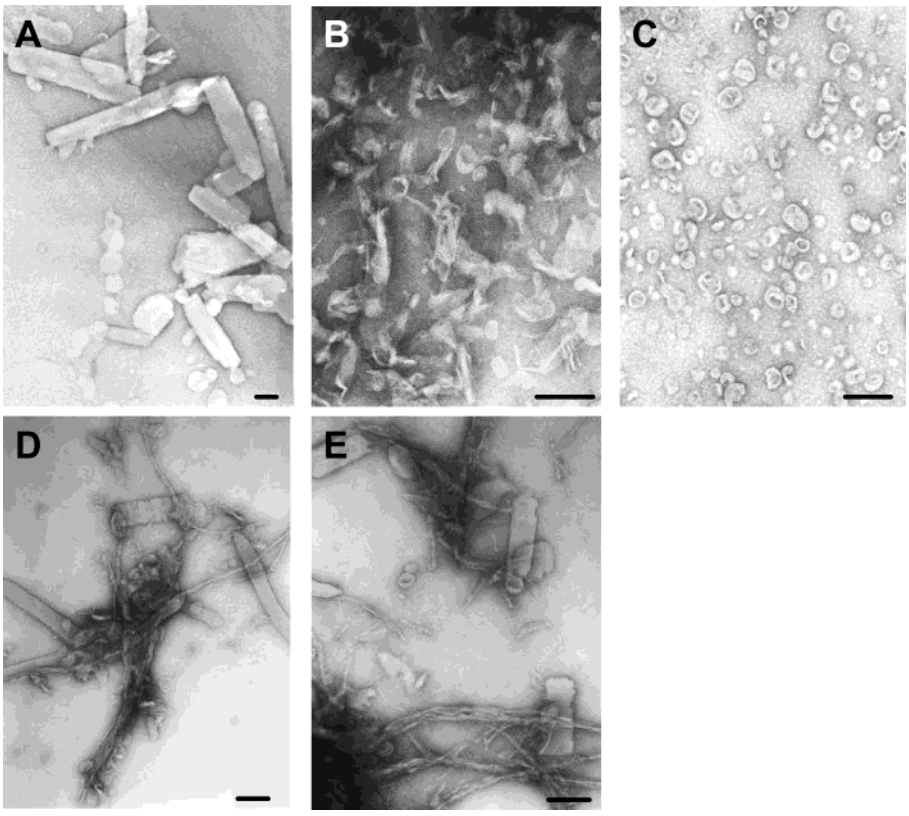

FIGURE 3: Ultrastructural morphology of lipid vesicles after addition of hIAPP. Vesicle samples (10 μL) used for the color reaction assay at various time points were negatively stained with uranyl acetate and visualized using transmission electron microscopy. (A) Control DMPC/PDA (2:3 mole ratio) vesicle sample, without addition of hIAPP. (B) DMPC/PDA vesicle after addition of a supernatant fraction incubated for 1 h. (C) DMPC/PDA vesicles after addition of 30 μM polymyxin B. (D) DMPC/PDA vesicles after addition of a supernatant fraction collected 4 h after the initial dissolution. (E) DMPC/PDA vesicles after addition of a pellet fraction collected 1 h after the initial dissolution. All scales are 100 nm in length.

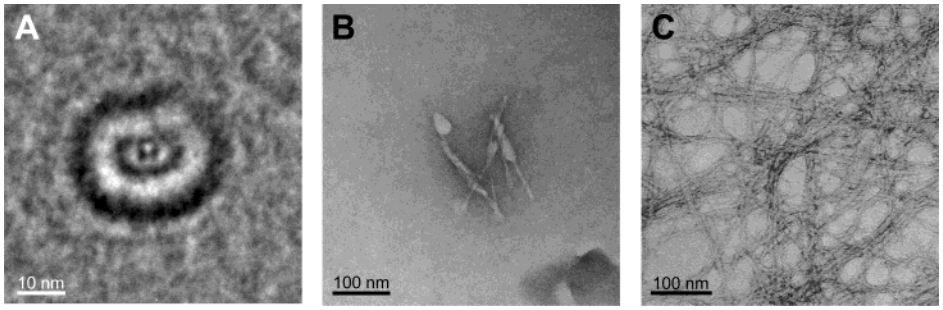

FIGURE 4: Ultrastructural morphology of hIAPP prefibrillar assemblies and mature fibrils. hIAPP was dissolved in HFIP and diluted in 10 mM acetate buffer (pH 6.5) to a final concentration of 4 μM and 1% HFIP. After 60 min, a sample was separated using centrifugation (20000*g*), and 10 μL of the supernatant was negatively stained with uranyl acetate and visualized using transmission electron microscopy (TEM) and high-resolution field-emission gun TEM (HR-TEM). (A) HR-TEM micrograph of a spheroid prefibrillar assembly, 20 nm in diameter, present in the supernatant fraction after 60 min. (B) TEM micrograph of protofibrils (an initiation of elongated fibrils) present in the supernatant fraction after 60 min. (C) TEM micrograph of mature hIAPP fibrils after 24 h. The sample was visualized without separation through centrifugation.

potent membrane-disrupting antimicrobial peptide (Figure 3C). A similar degradation of phospholipid/PDA vesicles following lipid disruption by various membrane-reactive compounds was previously observed (S. Kolusheva and R. Jelinek, unpublished results).

Significantly different appearances were detected in the vesicle samples following addition of a supernatant fraction collected 4 h after the initial dissolution (Figure 3D) or a pellet suspension 60 min after peptide dissolution (Figure 3E). Both images clearly feature elongated fibrils, some attached to the rectangular lipid/PDA particles. Importantly, the vesicles did not appear to be disrupted or deformed by the fibrils, in contrast to the apparent pronounced degradation following addition of the supernatant suspension extracted after 1 h (Figure 3B).

To gain a better understanding of the morphology of the soluble prefibrillar assemblies present in the supernatant solution, we used high-resolution TEM analysis (HR-TEM) to visualize the soluble fraction after 60 min without the addition of lipid vesicles (Figure 4). Synthetic hIAPP was dissolved, separated using centrifugation, and visualized after 60 min. The supernatant fraction of the peptide contained spheroid assemblies, 15−20 nm in diameter (Figure 4A) with a morphology very similar to that of early assemblies that were observed with the β-amyloid polypeptide (*20*). TEM analysis of the supernatant fraction further revealed the early stages of fibrillar assemblies, or in the more common term "protofibril assemblies" (Figure 4B). The protofibrillar assemblies exhibited different morphologies as compared with the mature fibrils (Figure 4C), having less distinct contours of thicker and shorter assemblies.

The TEM analysis provides clear visual evidence for the membrane activity of the transient prefibrils assembled in the hIAPP suspensions, reaching their maximal activity approximately 1 h after the dissolution of the peptide in aqueous solutions.

Secondary Structure Analysis of Membrane−hIAPP Complexes Using CD. To further evaluate the correlation between the structural properties of the hIAPP assemblies and their membrane interactions, we recorded CD spectra of the peptide−suspension supernatants extracted at different time points, after mixing with the lipid/PDA vesicles (Figure 5). hIAPP has been shown to adopt a random-coil conformation in aqueous solutions, transforming slowly into a β-sheet structure (*19*). In the presence of lipid/PDA vesicles,

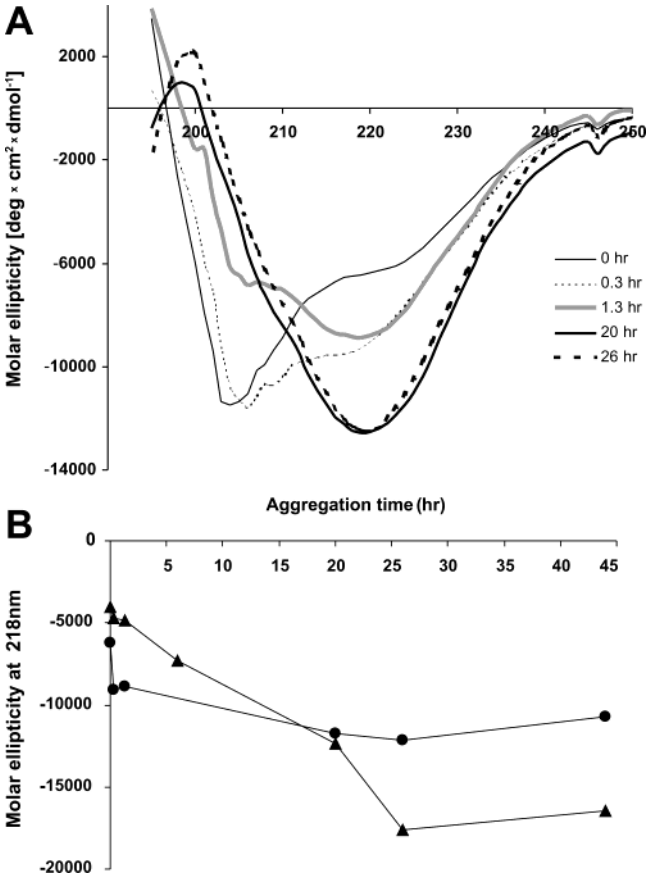

FIGURE 5: Secondary structure analysis of lipid vesicles and hIAPP using CD spectroscopy. hIAPP (4 μM) was dissolved in 10 mM sodium acetate buffer (pH 6.5) and 1% HFIP. (A) CD spectra of hIAPP in the presence of 50 mM DMPC/PDA vesicles. Peptide samples were collected after the indicated incubation times. (B) Molar ellipticity at 218 nm (corresponding to formation of β-sheet structures) of hIAPP in an aqueous solution (▲) and hIAPP in a solution containing DMPC/PDA vesicles (●).

however, we observed that the transition from a random coil to a β-sheet structure was already apparent after only 20 min, becoming the dominant peptide structure after little more than 1 h (Figure 5A).

A comparison of the molar ellipticity values of hIAPP and an hIAPP/lipid/PDA vesicle mixture at 218 nm (Figure 5B) clearly shows that β-sheet formation was significantly enhanced shortly after peptide dissolution in the presence of the vesicles. Figure 5B shows that the molar ellipticity of

hIAPP decreased rapidly to approximately −10000 deg cm^2 dmol^{-1} when the peptide was suspended with the vesicles, while a much slower adoption of a sheet structure was apparent in a vesicle-free aqueous solution (Figure 5B). The CD spectral analysis thus confirms that significant membrane binding occurs for prefibrillar assemblies formed in the peptide suspension within approximately 1 h, giving rise to the expected β-sheet structures.

DISCUSSION

The formation of amyloid fibrils is a hallmark of a variety of seemingly unrelated diseases. Despite their central importance in public health, the mechanism of amyloid-related pathogenesis is not fully understood. A thorough mechanistic understanding of the pathogenesis process would be important both for the basic understanding of the phenomenon and for the development of future therapeutic approaches.

In this work, we provide convincing experimental evidence for the existence of transient soluble membrane-active intermediate hIAPP species which appear in aqueous solutions prior to fibril formation. The observation of a gradual increase in the extent of lipid bilayer perturbation reaching a maximum after approximately 1 h is a clear indication that membrane interactions are not mediated by monomeric hIAPP but rather that a process of assembly is necessary for the formation of membrane-active species. Furthermore, the progressive decrease in the extent of membrane interactions after the peak after incubation for 1 h (Figures 1 and 2) as well as the detection of membrane activity only in the supernatant fractions suggests that the transient assemblies consist of prefibrillar assemblies rather than the large fibrillar structures.

The ultrastructural TEM analyses in Figures 3 and 4 provided observable evidence for the existence of prefibrillar assemblies and their morphologies. The electron microscopy data indicated the formation of spherical prefibrillar assemblies, 1 h after IAPP solubilization, and demonstrated the transformation of these assemblies into elongated mature fibrils (Figure 4). The appearance of soluble spherical assemblies with a very similar ultrastructure was previously reported for other amyloidogenic proteins such as β-amyloid and α-synuclein (*20*, *39*, *40*) and is consistent with a pore formation mechanism of toxicity (*20*).

Detection of rapid formation of β-sheet structures upon association with the lipid/PDA vesicles (Figure 5) is a further indication for the enhanced membrane interactions of the transient prefibrillar assemblies. Importantly, the assembly of amyloid fibrils *in vivo* occurs in the intracellular space, in which cellular membranes are readily accessible for molecular interactions.

Our observation of membrane interaction and bilayer disruption induced by prefibrillar assemblies of amyloidogenic polypeptides is highly relevant for the development of therapeutic agents aimed at preventing and treating amyloid-related diseases. Indeed, the emerging molecular mechanism of amyloid toxicity suggests that the disassembly of the larger fibrils that were already formed may be actually more harmful than beneficial. This is because amyloid fibril disruption might actually result in an increased concentration of monomeric peptides and prefibrils that will exert higher cytotoxic activity. According to our study, a therapeutic effort might be better directed toward inhibition of the earlier stage of transient prefibril formation. This could be achieved by targeting the molecular recognition determinants that may play a role in the very early stages of oligomerization. We have recently determined such a molecular recognition site within the IAPP molecule by an exhaustive nonbiased peptide array screen (*33*). The apparent role of aromatic interactions in the molecular recognition and self-assembly of IAPP (*33*−*35*) and other amyloidogenic polypeptides (*36*−*38*) may point to specific design criteria leading to inhibitors that will target the early stages of molecular association leading to formation of prefibrillar assemblies.

ACKNOWLEDGMENT

We thank Y. Delarea for his help with TEM experiments, Dr. Y. Lereah for his help with HR-TEM experiments, and members of the Gazit laboratory for helpful discussions.

REFERENCES

1. Wetzel, R. (1996) *Cell 86*, 699−702.
2. Rochet, J. C., and Lansbury, P. T., Jr. (2000) *Curr. Opin. Struct. Biol. 10*, 60−68.
3. Dobson, C. M. (2001) *Philos. Trans. R. Soc. London, Ser. B 356*, 133−145.
4. Sacchettini, J. C., and Kelly, J. W. (2002) *Nat. Rev. Drug Discovery 1*, 267−275.
5. Gazit, E. (2002) *Curr. Med. Chem. 9*, 1725−1735.
6. Höppener, J. W., Ahrén, B., and Lips, C. J. (2000) *N. Engl. J. Med. 343*, 411−419.
7. Höppener, J. W., Oosterwijk, C., Nieuwenhuis, M. G., Posthuma, G., Thijssen, J. H., Vroom, T. M., Ahrén, B., and Lips, C. J. (1999) *Diabetologia 42*, 427−434.
8. Kahn, S. E. (2003) *Diabetologia 46*, 3−19.
9. Gebre-Medhin, S., Olofsson, C., and Mulder, H. (2000) *Diabetologia 43*, 687−695.
10. Jarrett, J. T., and Lansbury, P. T., Jr. (1992) *Biochemistry 31*, 12345−12352.
11. Kayed, R., Bernhagen, J., Greenfield, N., Sweimeh, K., Brunner, H., Voelter, W., and Kapurniotu, A. (1999) *J. Mol. Biol. 287*, 781−796.
12. Padrick, S. B., and Miranker, A. D. (2002) *Biochemistry 41*, 4694−4703.
13. Gazit, E. (2002) *Angew. Chem., Int. Ed. 114*, 267−269.
14. Bucciantini, M., Giannoni, E., Chiti, F., Baroni, F., Formigli, L., Zurdo, J., Taddei, N., Ramponi, G., Dobson, C. M., and Stefani, M. (2002) *Nature 416*, 507−511.
15. Lorenzo, A., Razzaboni, B., Weir, G. C., and Yankner, B. A. (1994) *Nature 368*, 756−760.
16. MacGibbon, G. A., Cooper, G. J., and Dragunow, M. (1997) *Neuroreport 8*, 3945−3950.
17. Saafi, E. L., Konarkowska, B., Zhang, S., Kistler, J., and Cooper, G. J. S. (2001) *Cell Biol. Int. 25*, 339−350.
18. Zhang, Z., Liu, J., MacGibbon, G. A., Dragunow, M., and Cooper, G. J. (2002) *J. Mol. Biol. 324*, 271−285.
19. Anguiano, M., Nowak, R. J., and Lansbury, P. T., Jr. (2002) *Biochemistry 41*, 11338−11343.
20. Lashuel, H. A., Hartley, D., Petre, B. M., Walz, T., and Lansbury, P. T., Jr. (2002) *Nature 418*, 291.
21. Harper, J. D., Wong, S. S., Lieber, C. M., and Lansbury, P. T., Jr. (1999) *Biochemistry 38*, 8972−8980.
22. Chiti, F., Bucciantini, M., Capanni, C., Taddei, N., Dobson, C. M., and Stefani, M. (2001) *Protein Sci. 10*, 2541−2547.
23. El-Agnaf, O. M., Nagala, S., Patel, B. P., and Austen, B. M. (2001) *J. Mol. Biol. 310*, 157−168.
24. Kayed, R., Head, E., Thompson, J. L., McIntire, T. M., Milton, S. C., Cotman, C. W., and Glabe, G. C. (2003) *Science 300*, 486−489.
25. Kolusheva, S., Shahal, T., and Jelinek, R. (2000) *Biochemistry 39*, 15851−15859.
26. Kolusheva, S., Kafri, R., Katz, M., and Jelinek, R. (2001) *J. Am. Chem. Soc. 123*, 417−422.
27. Jelinek, R., and Kolusheva, S. (2001) *Biotechnol. Adv. 19*, 109−118.

28. Jelinek, R., Okada, S., Norvez, S., and Charych, D. (1998) *Chem. Biol. 5*, 619−629.
29. Ahn, T., Oh, D. B., Lee, B. C., and Yun, C. H. (2000) *Biochemistry 39*, 10147−10153.
30. Kolusheva, S., Wachtel, E., and Jelinek, R. (2003) *J. Lipid Res. 44*, 65−71.
31. Satchell, D. P., Sheynis, T., Shirafuji, Y., Kolusheva, S., Ouellette, A. J., and Jelinek, R. (2003) *J. Biol. Chem. 278*, 13838−13846.
32. Langner, M., and Hui, S. W. (1993) *Chem. Phys. Lipids 65*, 23−30.
33. Mazor, Y., Gilead, S., Benhar, I., and Gazit, E. (2002) *J. Mol. Biol. 322*, 1013−1024.
34. Azriel, R., and Gazit, E. (2001) *J. Biol. Chem. 276*, 34156−34161.
35. Porat, Y., Stepensky, A., Ding, F.-X., Naider, F., and Gazit, E. (2003) *Biopolymers 69*, 161−164.
36. Gazit, E. (2002) *FASEB J. 16*, 77−83.
37. Reches, M., Porat, Y., and Gazit, E. (2002) *J. Biol. Chem. 277*, 35475−35480.
38. Reches, M., and Gazit, E. (2003) *Science 300*, 625−627.
39. Goldberg, M. S., and Lansbury, P. T., Jr. (2000) *Nat. Cell Biol. 2*, E115−E119.
40. Hoshi, M., Sato, M., Matsumoto, S., Noguchi, A., Yasutake, K., Yoshida, N., and Sato, K. (2003) *Proc. Natl. Acad. Sci. U.S.A.* 100, 6370−6375.

BI034889I